MOLECULAR AND CELLULAR BIOLOGY, July 2004, p. 5776–5787 Vol. 24, No. 13
0270-7306/04/$08.00+0 DOI: 10.1128/MCB.24.13.5776–5787.2004

The Structure-Specific Endonuclease Ercc1-Xpf Is Required To Resolve DNA Interstrand Cross-Link-Induced Double-Strand Breaks

Laura J. Niedernhofer,[1]* Hanny Odijk,[1] Magda Budzowska,[1] Ellen van Drunen,[1] Alex Maas,[1] Arjan F. Theil,[1] Jan de Wit,[1] N. G. J. Jaspers,[1] H. Berna Beverloo,[1] Jan H. J. Hoeijmakers,[1] and Roland Kanaar[1,2]

Departments of Cell Biology and Genetics[1] and Radiation Oncology,[2] Erasmus Medical Center, 3000 DR Rotterdam, The Netherlands

Received 6 December 2003/Returned for modification 7 January 2004/Accepted 6 April 2004

Interstrand cross-links (ICLs) are an extremely toxic class of DNA damage incurred during normal metabolism or cancer chemotherapy. ICLs covalently tether both strands of duplex DNA, preventing the strand unwinding that is essential for polymerase access. The mechanism of ICL repair in mammalian cells is poorly understood. However, genetic data implicate the Ercc1-Xpf endonuclease and proteins required for homologous recombination-mediated double-strand break (DSB) repair. To examine the role of Ercc1-Xpf in ICL repair, we monitored the phosphorylation of histone variant H2AX (γ-H2AX). The phosphoprotein accumulates at DSBs, forming foci that can be detected by immunostaining. Treatment of wild-type cells with mitomycin C (MMC) induced γ-H2AX foci and increased the amount of DSBs detected by pulsed-field gel electrophoresis. Surprisingly, γ-H2AX foci were also induced in *Ercc1*$^{-/-}$ cells by MMC treatment. Thus, DSBs occur after cross-link damage via an Ercc1-independent mechanism. Instead, ICL-induced DSB formation required cell cycle progression into S phase, suggesting that DSBs are an intermediate of ICL repair that form during DNA replication. In *Ercc1*$^{-/-}$ cells, MMC-induced γ-H2AX foci persisted at least 48 h longer than in wild-type cells, demonstrating that Ercc1 is required for the resolution of cross-link-induced DSBs. MMC triggered sister chromatid exchanges in wild-type cells but chromatid fusions in *Ercc1*$^{-/-}$ and Xpf mutant cells, indicating that in their absence, repair of DSBs is prevented. Collectively, these data support a role for Ercc1-Xpf in processing ICL-induced DSBs so that these cytotoxic intermediates can be repaired by homologous recombination.

Interstrand cross-links (ICLs) comprise a unique class of DNA lesions that have a potent biological effect. By definition, ICLs involve covalent modification of both strands of DNA. Therefore, these adducts prevent DNA strand separation and block DNA metabolism, such as transcription and replication (31). DNA-damaging agents that cause ICLs are extremely cytotoxic, and their utility as anticancer chemotherapeutics likely stems from their selective toxicity to proliferating cells. ICLs occur via a two-step reaction mechanism in which first a monoadduct involving one strand of DNA is formed (24). Although cross-linking agents induce a variety of DNA adducts, the relative cytotoxicity of each agent correlates with its ability to form ICLs (43, 44).

The repair of DNA ICLs presents a unique challenge to cells. Since both strands of DNA are covalently modified, simple excision of the lesion followed by template-driven DNA resynthesis is precluded. In *Escherichia coli*, two solutions to this problem have been identified (reviewed in reference 19). In both these repair mechanisms, the ICL is excised from one strand. In error-free repair, an undamaged chromosome is then utilized as a template for gap-filling DNA polymerization (55). ICL repair also occurs in recombination-deficient *E. coli*, likely via translesional DNA polymerization of the second damaged strand (5). Similarly, genetic analysis of *Saccharomyces cerevisiae* (23) and mammalian DNA repair mutants (reviewed in reference 19) indicates the involvement of proteins from multiple DNA repair pathways in ICL repair: nucleotide excision repair (NER), homologous recombination, and postreplication repair.

An interesting difference in ICL repair between *S. cerevisiae* and higher eukaryotes is that in mammals, not all NER mutants are equally sensitive to ICLs (19). *Xpf* and *Ercc1* mutants are much more sensitive than *Xpa* mutants. In cells, the Xpf and Ercc1 proteins heterodimerize (7, 59) to form a structure-specific endonuclease that nicks double-stranded DNA adjacent to a 3′ single-strand region (4). Ercc1-Xpf is responsible for incising the damaged strand of duplex DNA 5′ to a lesion in NER of monoadducts (41, 54). A second endonuclease with opposite polarity (Xpg) is required for complete excision of a damaged oligonucleotide during NER (35). Furthermore, Xpa is required to recruit Ercc1-Xpf to the site of DNA damage (60), and the presence of Xpg is required for Ercc1-Xpf catalytic activity in NER (61), yet neither *Xpa* nor *Xpg* mutants are as sensitive to ICL damage as *Xpf* and *Ercc1* mutants (17). Thus, ICL repair is distinct from NER in eukaryotes, and complete removal of an ICL likely necessitates a second nuclease, in addition to Ercc1-Xpf, that can incise 3′ to the lesion.

Also in contrast to prokaryotes, there is evidence in eukaryotes that ICLs elicit double-strand breaks (DSBs) (9, 12,

* Corresponding author. Present address: University of Pittsburgh Cancer Institute, Hillman Cancer Center 2.6, 5117 Centre Ave., Pittsburgh, PA 15213-1863. Phone: (412) 623-7763. Fax: (412) 623-7761. E-mail: niedernhoferl@upmc.edu.

17, 33, 37). Thus, it has been proposed that in mammalian cells ICL repair proceeds via the formation of a DSB, with subsequent repair of the DSB occurring by homologous recombination (6, 17, 29). Such models are consistent with the fact that cells deficient in Rad51 paralogues or other proteins involved in homologous recombination-mediated DSB repair are sensitive to agents that induce DNA ICLs (17, 19). In addition, there is evidence that Ercc1-Xpf participates in certain homologous recombination pathways in eukaryotes (27, 42, 51–53). In *Saccharomyces cerevisiae*, *rad1* and *rad10* are epistatic in relation to mitotic recombination (53), suggesting that heterodimerization and therefore likely endonuclease activity are required for recombination. Indeed, Rad1-Rad10 cleaves nonhomologous single-strand ends from DSBs to facilitate repair via homologous recombination in *S. cerevisiae* (21, 45), as do the hamster homologues (1).

In this study, we investigated the role of Ercc1-Xpf in DNA ICL repair by using immunodetection of histone variant γ-H2AX to visualize DSBs in the nuclei of cells (47). H2AX is a histone that is specifically phosphorylated at Ser139 upon DSB induction (40, 48). This modification accumulates at sites of DNA DSBs, yielding discrete foci at breaks detected by immunostaining with an antibody against the phosphoepitope (47). Our results reveal that Ercc1-Xpf is not required for the formation of DSBs after cross-link damage but is imperative for their resolution.

MATERIALS AND METHODS

Cell lines. The generation, characterization, and culturing of *Ercc1*$^{-/-}$ embryonic stem (ES) cells have been described previously (42). Primary mouse embryonic fibroblast (MEF) lines were developed from day 13.5 embryos from either *Ercc1*$^{+/-}$ or *Xpa*$^{+/-}$ crossings as described previously (64). The genetic background was either C57BL/6 or FVB/n. Genomic DNA was isolated from a tissue sample of each embryo after overnight digestion with proteinase K in 50 mM Tris-HCl (pH 7.5)–100 mM EDTA–100 mM NaCl–1% sodium dodecyl sulfate. Genotyping of the *Ercc1* allele was done by PCR coamplification of intron 7 from the wild-type allele and the 3′ end of the selectable neomycin resistance marker from the targeted allele with a combination of primers specific for exons 7 and 8 of *Ercc1* and *neo*^{r} (5′-GAAAAGCTGGAGCAGAACTT, 5′-AGATTTCACGGTGGTCAGAC, and 5′-GAAGAGCTTGGCGGCGA ATG, respectively) (64). Genotyping of the *Xpa* allele was also done by PCR (18). MEFs were cultured in a 1:1 mix of Dulbecco's modified Eagle's medium and Ham's F10 with 10% fetal calf serum and antibiotics. Each experimental replica was done with a new MEF line, created from a unique embryo, in its second or third passage. Cell lines derived from wild-type littermates were used as controls in all experiments.

Immunofluorescence. Cells were trypsinized and seeded at approximately 25% confluence on glass coverslips. For ES cells, the glass was coated with gelatin. Sixteen hours later, the cells were irradiated with γ rays (10 Gy) or UV-C (254 nm, 10 J/m^2). For other experiments, the wild-type and mutant cells were exposed for 1 h to equitoxic doses of mitomycin C (MMC) or cisplatin, with doses giving 10% survival. For MEFs, the concentrations were 3 and 1 μM MMC for wild-type and mutant cells, respectively. For ES cells, 3 μM and 300 nM MMC were used. For exposure of ES cells to cisplatin, 13.3 and 3.3 μM concentrations of the drug were used for wild-type and Ercc1-deficient cells, respectively. Afterwards, the cells were washed and incubated in fresh medium at 37°C for the indicated amount of time and then fixed with 2% paraformaldehyde in sodium phosphate buffer, pH 7.4, for 15 min. Cells were permeabilized with 0.1% Triton X-100 in phosphate-buffered saline, and the phosphorylated form of H2AX (γ-H2AX) was detected with polyclonal anti-γ-H2AX (1:1,000; Upstate Biotechnologies) and Alexa 488-conjugated goat anti-rabbit immunoglobulin (1:500; Molecular Probes) in phosphate-buffered saline with 0.15% glycine and 0.5% bovine serum albumin. Nuclear staining patterns were visualized with a Leica DMRB fluorescent microscope and fluorescein isothiocyanate filter at 40 to 100× magnification. For cell cycle arrest in G_1, cells were treated with DNA-damaging agents 48 h after reaching confluence. Duplicate plates of the cells were subsequently released from arrest by trypsinization and reseeding on coverslips at low cell density.

Detection of DSBs by pulsed-field gel electrophoresis. Subconfluent cultures of wild-type and *Ercc1*$^{-/-}$ ES cells were treated with 7.2 μM MMC for 1 h. Afterwards, the cells were washed extensively with phosphate-buffered saline and incubated with fresh medium for 6 to 48 h. Cells were harvested by trypsinization, and agarose plugs of 5×10^6 cells were prepared with a CHEF disposable plug Mold (Bio-Rad). The samples were lysed with proteinase K (1 mg/ml in100 mM EDTA–0.2% sodium deoxycholate–1% sodium lauryl sarcosine) for 48 h at 50°C and then washed repetitively with Tris-EDTA. The plugs were electrophoresed for 23 h at 13°C in 0.9% agarose and 250 mM Tris-borate-EDTA with a Biometra Rotaphor apparatus with the following parameters: interval, 30 to 5 s log; angle, 120 to 110° linear; 180 to 120 V log). The gels were stained with ethidium bromide for 5 h and then destained for 16 h in 250 mM Tris-borate-EDTA, and the DNA was visualized with a Typhoon 9200 scanner (Amersham Pharmacia Biotech).

Flow cytometric analysis. Subconfluent cultures of early-passage primary MEFs or ES cells were exposed for 1 h to equitoxic concentrations of MMC as indicated above. The cells were then washed and grown for an additional 12 h, at which point they were harvested by trypsinization, fixed in 70% ethanol, and stained with propidium iodide. The DNA content of the cells was determined by fluorescence-activated cell sorting (FACS) using a Facscan (Becton Dickinson). The fraction of cells in each phase of the cell cycle was calculated with CellQuest.

Chromosome and sister chromatid exchange analysis. Wild-type (CHO9 and AA8) and mutant (CHO43-3B for *Ercc1* and UV47 for *Xpf*) Chinese hamster ovary (CHO) and murine ES cells were exposed for 1 h to equitoxic doses of cisplatin or MMC corresponding to 10% survival and then washed, and the medium was exchanged for one containing bromodeoxyuridine (BrdU; 10 μg/ml). Cultures were grown for an additional 24 h, and the cells were harvested by trypsinization and prepared for metaphase analysis as previously described (20). Nuclei were scored as being in either the first or second metaphase division, based on the differential staining pattern of sister chromatids with acridine orange as a fluorescent stain. The number of aberrations per metaphase was counted, and the aberrations were classified as chromatid type, chromosome aberrations, or structures resulting from fusions.

RESULTS

Detection of DSBs after DNA damage. To determine if processing of DNA ICLs causes genomic DSBs, proliferating cultures of wild-type primary MEFs were plated on glass coverslips, exposed to various DNA-damaging agents, and then fixed and stained for the phosphoepitope of H2AX (γ-H2AX). Untreated cells displayed a homogenous nuclear staining, with a fraction of cells containing either one or two foci or >10 foci (Fig. 1A, first panel). As expected, when DSBs were induced with γ-irradiation, the γ-H2AX staining revealed a punctate pattern of >10 foci in virtually every nucleus (Fig. 1A, middle panel) (47). Foci of γ-H2AX were also induced in the majority of cells by MMC, a DNA ICL-inducing agent (Fig. 1A, last panel), demonstrating that DSBs are indeed a consequence of ICL damage. These data support previous reports of ICL-dependent DSBs in yeast and mammalian cells detected by alkaline elution (9, 33) and pulsed-field gel electrophoresis (12, 13, 17, 37).

At the concentration of MMC used (3 μM), the number of ICLs is approximated to be on the order of 10^3 per genome (44, 63). However, the maximum number of foci detected was two orders of magnitude lower, reflecting either an inefficient yield of DSBs from ICLs or the relatively low resolution of this technique (47). γ-H2AX foci were also observed in wild-type ES cells treated with MMC (Fig. 1B). Thus, DSB formation is not a cell type-specific event. In contrast to MMC, UV-C irradiation, which causes intrastrand cross-links, did not elicit the formation of prominent γ-H2AX foci at the dose used (Fig. 1B) (46). We conclude that DSB formation is a specific con-

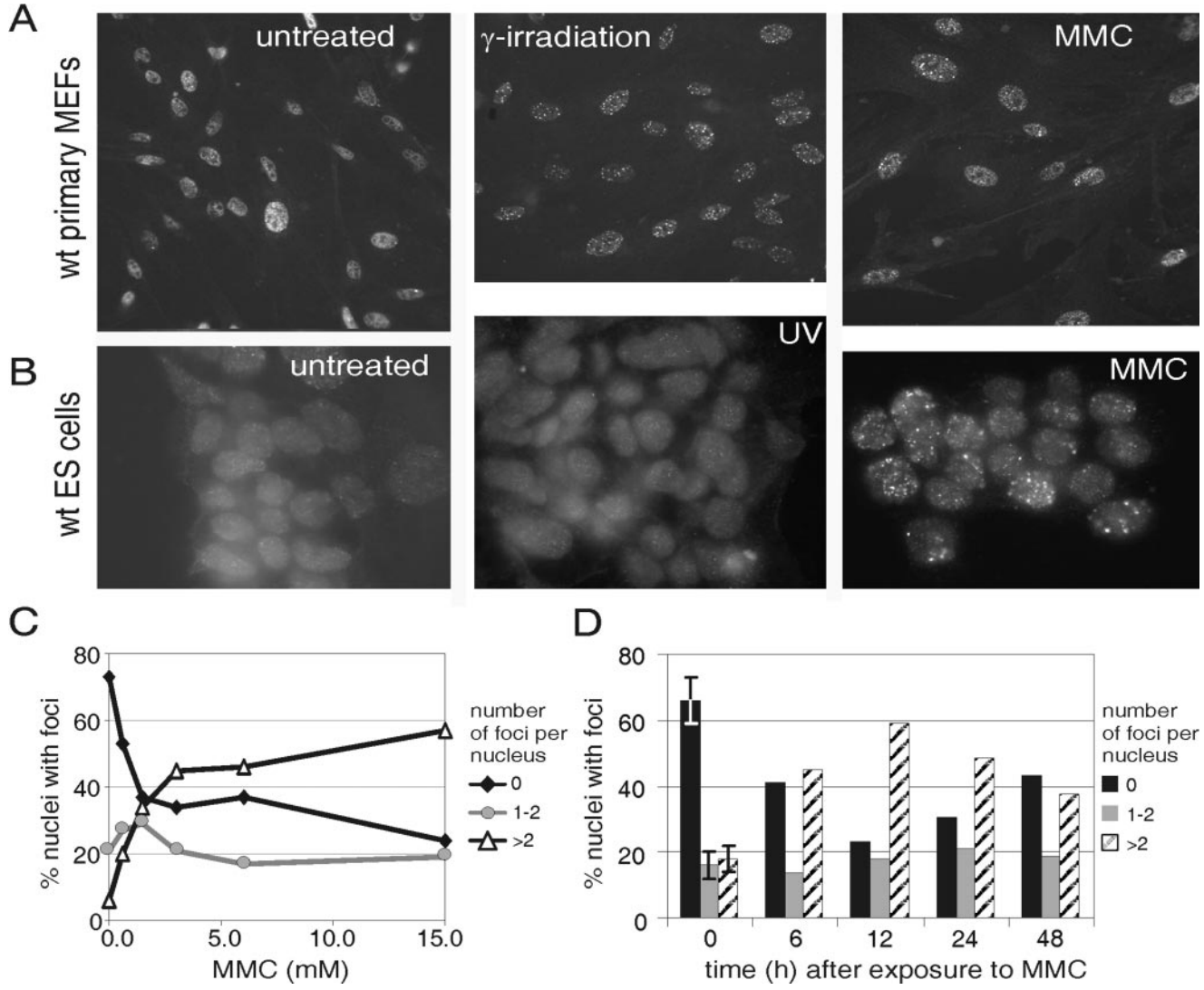

FIG. 1. γ-H2AX foci in wild-type cells after DNA damage. (A) Early-passage wild-type (wt) primary MEFs were seeded on glass coverslips at low cell density. After 16 h, the cells were exposed to 10 Gy of γ-irradiation or to 3 μM MMC for 1 h and then further incubated at 37°C. Ten hours later, the cells were fixed and immunostained for γ-H2AX. (B) Wild-type murine ES cells were seeded on gelatin-coated glass coverslips and after 16 h exposed to UV-C (254 nm, 10 J/m^2) or 3 μM MMC for 1 h. The cells were cultured for an additional 14 h and then fixed and processed as described for panel A. (C) Quantitation of γ-H2AX foci after exposure of cells to increasing concentrations of MMC. Early-passage wild-type primary MEFs seeded on glass coverslips were exposed to a range of concentrations of MMC for 1 h and then grown in fresh medium for 12 h prior to fixation and immunostaining for γ-H2AX. For each data point, more than 100 nuclei were examined, the γ-H2AX foci were counted, and the cells were categorized as having zero, one to two, or more than two foci per nucleus. The percentage of cells in each category is plotted. (D) Quantitation of γ-H2AX focus formation at various time points after exposure of wild-type cells to 3 μM MMC. Error bars indicate the standard error of the mean when the data were collected from more than three individual experiments.

sequence of processing DNA ICLs but not intrastrand cross-links.

Quantitation of DSBs after cross-link damage. To quantitate DSB formation after MMC treatment, the number of γ-H2AX foci in each cell was counted and the cells were categorized as having zero, one to two, or more than two foci per nucleus. Spontaneous foci were detected in 30% of wild-type MEFs (Fig. 1C and D). Half of these cells had only one to two foci each, likely reflecting unrepaired, spontaneous DNA damage. The other half of the cells had an average of >10 γ-H2AX foci. These are likely cells that were in, or recently emerged from, S phase at the time of fixation (22, 39, 46, 47). Accordingly, the fraction of cells with more than two spontaneous foci approximates the fraction of primary MEFs that were not in the G_1 phase of the cell cycle in an unsynchronized culture (see Fig. 3) (28).

At the lowest dose of MMC tested (0.6 μM), there was a 20% decrease in the number of fibroblasts with no γ-H2AX foci, while the fraction of cells with either one to two or more than two foci increased proportionally (Fig. 1C). At higher concentrations of MMC, not only did the percentage of cells with foci continue to increase, but the number of foci per nucleus also increased, so that the fraction of cells with more than two foci exceeded the fraction of cells with only one to

two foci. Thus, DSB formation after ICL damage is dose dependent. At MMC concentrations above 3 μM, there was no further increase in the fraction of cells with foci. The observation that only ~60% of an unsynchronized population of fibroblasts responded to MMC-induced damage within a 12-h period provides an indication that DSB formation might require cell cycle progression.

The time course of γ-H2AX focus formation further supports this conclusion (Fig. 1D). We detected no appreciable increase in the fraction of cells with foci until 6 h after exposure to the saturating dose of MMC (3 μM; data not shown). At 12 h, the fraction of cells with foci peaked and subsequently declined, most likely due to DSB repair. This is in striking contrast to the kinetics of γ-irradiation-induced γ-H2AX focus formation and resolution. γ-Irradiation inflicts DSBs directly, and γ-H2AX foci are detected immediately. Their number peaks within minutes of irradiation and begins to decline within 15 min (47). Thus, DSB formation after cross-link damage is clearly indirect and possibly linked to cell cycle progression.

Detection of DSBs after DNA damage of *Ercc1*$^{-/-}$ cells. To determine if Ercc1-Xpf endonuclease is required for the creation of ICL-dependent DSBs, we investigated whether γ-H2AX foci would form in Ercc1-deficient cells after exposure to various ICL-inducing agents. In contrast to wild-type cells, analysis of untreated *Ercc1*$^{-/-}$ primary MEFs revealed a high frequency of nuclei with one to two spontaneous γ-H2AX foci (Fig. 2A, first panel), suggesting a higher steady-state level of unrepaired DNA damage in the mutant cells. As in wild-type cells, γ-irradiation induced a dramatic increase in the number of γ-H2AX foci (Fig. 2A, middle panel). MMC also induced γ-H2AX focus formation in the *Ercc1*$^{-/-}$ MEFs (Fig. 2A, last panel). As with the wild-type cells, the response to MMC was not cell type specific but was specific for agents that cause DNA ICLs (Fig. 2B). Large numbers of γ-H2AX foci were induced not only by MMC but also by cisplatin, indicating that DSB formation is also not peculiar to a specific cross-linking agent. As in the mutant MEFs, *Ercc1*$^{-/-}$ ES cells had an increased incidence of spontaneous γ-H2AX foci compared to wild-type ES cells (Fig. 2B versus 1B), suggesting genomic instability or persistent endogenous DNA damage as a result of a mutation in *Ercc1*. We conclude that the formation of ICL-induced DSBs is Ercc1 independent.

Kinetics of γ-H2AX focus formation in *Ercc1*$^{-/-}$ MEFs. The number of γ-H2AX foci in *Ercc1*$^{-/-}$ MEFs after exposure to MMC at a concentration equitoxic to that used for wild-type cells was counted. Quantitation of foci in untreated *Ercc1*$^{-/-}$ cells revealed a significantly greater fraction of cells with one to two foci (35 ± 5%) than in untreated wild-type cells (16 ± 6%; Fig. 2C versus 1D), indicating a higher steady-state level of DSBs in the mutant cells. As in wild-type cells, by 12 h after exposure to MMC, the fraction of cells with more than two foci dominated. The peak percentage of *Ercc1*$^{-/-}$ cells with more than two foci approximated that of wild-type cells after exposure to MMC. Thus, the formation of DSBs in response to ICL damage is identical in wild-type and *Ercc1*$^{-/-}$ MEFs. Interestingly, once the MMC-induced γ-H2AX foci appeared in *Ercc1*$^{-/-}$ cells, they persisted (Fig. 2C). Up to 72 h after the induction of ICL damage, the percentage of cells with more than two foci remained elevated, whereas in wild-type cells, the fraction of nuclei with more than two foci began to decline within 12 h of reaching its zenith (Fig. 1D).

To confirm that the persistent γ-H2AX foci in the *Ercc1*$^{-/-}$ cells reflected DSBs, we analyzed genomic DNA from MMC-treated cells by pulsed-field gel electrophoresis (Fig. 2E). Increased amounts of lower-molecular-weight DNA were detected in wild-type and *Ercc1*$^{-/-}$ cell plugs beginning 6 h after MMC treatment, confirming that the accumulation of γ-H2AX foci coincides with the creation of DSBs. Analogous to the immunofluorescence results, the amount of DSBs detected by pulsed-field gel electrophoresis at 24 to 48 h after MMC treatment was substantially greater in *Ercc1*$^{-/-}$ cells than in wild-type cells. Together, these data demonstrate that DSBs are indeed an intermediate of cross-link repair and that Ercc1 is required for the resolution of ICL-induced DSBs.

To determine if this function was unique to Ercc1 or related to its role in NER, we repeated the immunofluorescence assay with *Xpa*$^{-/-}$ primary MEFs. In these NER-deficient cells, as in wild-type cells, the fraction of cells with more than two foci declined significantly within 36 h of reaching a maximum (Fig. 2D). These data demonstrate that Ercc1, but not NER, is required for the resolution of ICL-induced DSBs.

Cell cycle dependence of γ-H2AX focus formation. Since Ercc1-Xpf endonuclease is not required for the formation of DSBs after induction of ICLs, we sought to determine how these DSBs do occur. To test the possibility that DNA replication was involved, we looked for γ-H2AX focus formation in nonproliferating cells. Wild-type primary MEFs were seeded at a high cell density to arrest them in G_1 by contact inhibition. Under these conditions, MMC-induced γ-H2AX focus formation was significantly attenuated compared to that in asynchronous cells (Fig. 3A versus 1D). The fraction of cells without foci remained stable for 48 h after exposure to MMC. However, when we exposed nonproliferating cells to MMC, incubated them for 12 h, and then trypsinized and reseeded them at a low cell density to release their cell cycle block, γ-H2AX foci appeared (Fig. 3B). The fraction of cells with more than two foci was elevated at 9 and 12 h after trypsinization and then diminished by 36 h after release from cell cycle arrest. Thus, ICL-induced DSBs are only seen in actively cycling cells.

Cell cycle arrest by cross-link damage. Next we examined the impact of ICL damage on the cell cycle of primary MEFs and ES cells. Proliferating wild-type and *Ercc1*$^{-/-}$ cells were treated with equitoxic concentrations of MMC and then cultured for an additional 12 h, at which point the greatest number of cells have DSBs. The cells were analyzed for DNA content by FACS, and the percentage of cells in the various stages of the cell cycle was plotted (Fig. 3C to E). MMC induced a strong arrest in late $S/G_2/M$ of the cell cycle in wild-type ES cells (Fig. 3C). This arrest was even more profound in *Ercc1*$^{-/-}$ ES cells treated with MMC (Fig. 3D). Thus, the time point at which DSB incidence is maximal (12 h post-MMC treatment) coincides with a profound late $S/G_2/M$ cell cycle arrest, strongly implicating S-phase DNA replication in the creation of DSBs. The arrest in primary MEFs was much less dramatic (Fig. 3E), which is not surprising in that the proliferation rate of primary MEFs is about half that of ES cells.

Chromosomal aberrations induced by ICL damage. We sought to determine the consequence of ICLs at the chromo-

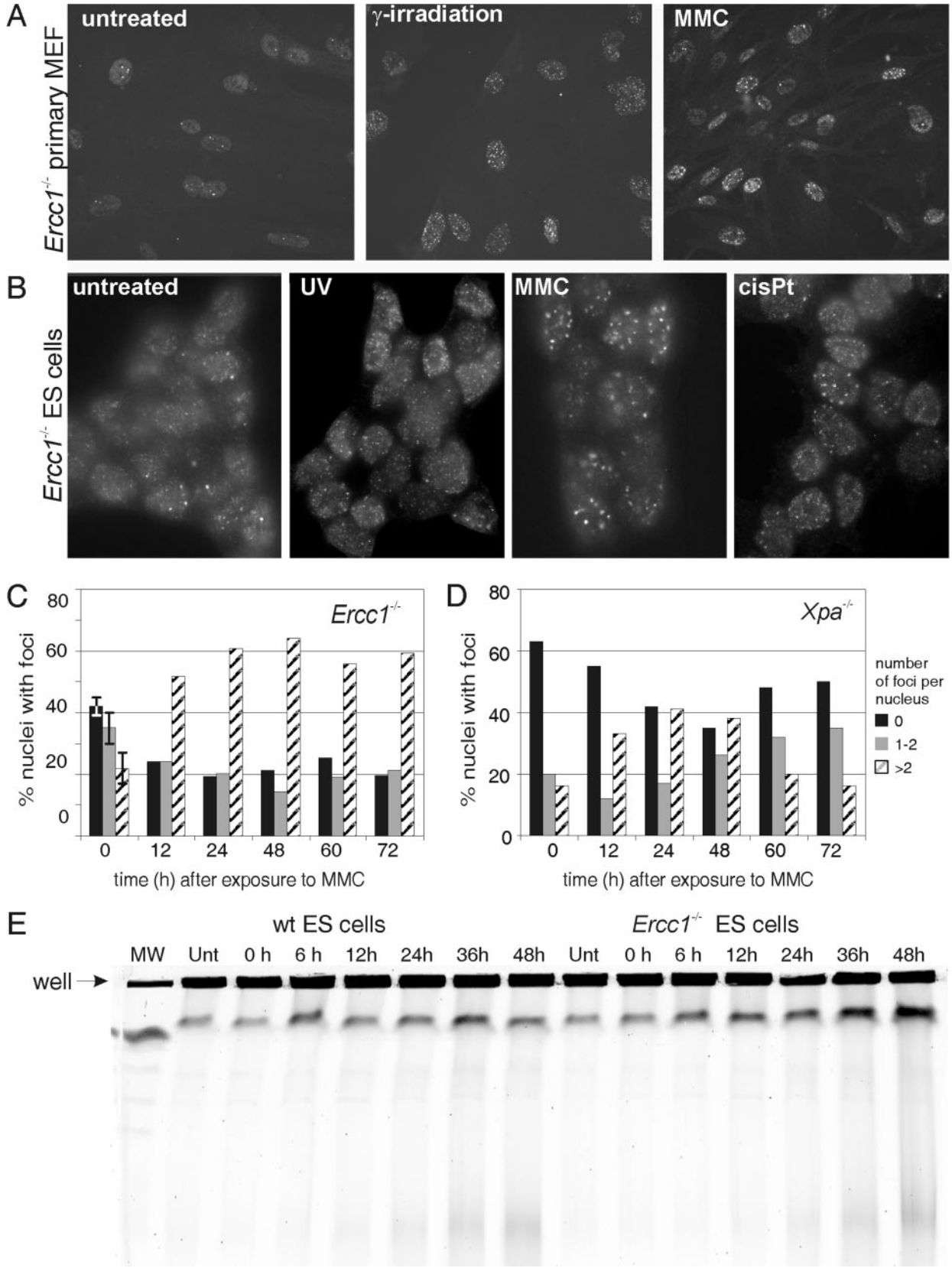

FIG. 2. γ-H2AX foci in *Ercc1*$^{-/-}$ cells after DNA damage. (A) Early-passage *Ercc1*$^{-/-}$ primary MEFs were seeded on glass as described for Fig. 1. DNA damage was induced with 10 Gy of γ-irradiation (equivalent dose to wild-type cells) or 1 μM MMC (equitoxic to wild-type cells) for 1 h. (B) *Ercc1*$^{-/-}$ ES cells were seeded on glass as described for Fig. 1. DNA damage was induced with UV-C at 10 J/m^2 (equivalent dose to

some level. Proliferating wild-type and *Ercc1*$^{-/-}$ ES cells were exposed to equitoxic concentrations of MMC for 1 h, and subsequently the medium was exchanged for one containing BrdU. After 24 h, the cells were harvested, and metaphase spreads were prepared. By examining the differential staining patterns of sister chromatids, the fraction of cells that had gone through either one or two S phases since the MMC treatment was determined. All of the metaphases from wild-type cells, with or without MMC exposure, had a staining pattern indicative of two rounds of replication in the presence of BrdU (Fig. 4A and Table 1). Chromosomal aberrations were rare and never complex. MMC induced an increased incidence of sister chromatid exchanges.

In contrast, in spreads prepared from *Ercc1*$^{-/-}$ ES cells treated with MMC, anaphase bridging and micronuclei were common (Fig. 4C), indicating chromatid nondisjunction. Only half of the *Ercc1*$^{-/-}$ cells exposed to MMC had reached the second division, demonstrating that the cell cycle delay in the mutant cells is substantially longer than in wild-type cells (Table 1). Furthermore, the metaphase spreads revealed a complex constellation of aberrations in response to MMC (Fig. 4B and Table 1). All metaphases arrested in the first division displayed numerous breaks, radial structures, and fusions. Interestingly, the majority of aberrations observed in wild-type and mutant cells were of the chromatid type, indicating that that their inception occurs during the previous S phase. None of the fusions observed were end to end, which was confirmed by detecting a full complementation of telomeres ($n = 40$) by fluorescent in situ hybridization with a telomere-specific probe (data not shown). Instead, all of the fusions were within the chromosomes, indicating the sites of unrepaired DSBs created during attempted replication of ICLs.

The same pattern of cell cycle arrest and chromosomal aberrations was observed with wild-type and *Ercc1* mutant CHO cells treated with cisplatin, reinforcing the idea that the observed results are neither cell type nor cross-linking agent specific (Fig. 4E, F, and G and Table 1). Furthermore, an *Xpf* mutant CHO cell line was studied, and it behaved identically to Ercc1-deficient cell lines (Fig. 4E and Table 1), extending these observations to both components of the Ercc1-Xpf endonuclease complex.

DISCUSSION

ICL-induced DSB formation is Ercc1 independent. To investigate the mechanism of DNA ICL repair in mammalian cells and to elucidate the role of the endonuclease Ercc1-Xpf, we studied the formation of DSBs in wild-type and Ercc1-Xpf-deficient cells treated with cross-linking agents by γ-H2AX immunodetection. We discovered that γ-H2AX foci form specifically in response to damaging agents that cause DNA ICLs and that these foci reflect genomic DSBs (Fig. 1 and 2). γ-H2AX focus formation after MMC damage is dose dependent and time dependent (Fig. 1C and D), strongly suggesting that DSBs are an intermediate of ICL repair. Interestingly, γ-H2AX foci also form in response to ICL damage in Ercc1-deficient cells (Fig. 2A and B). These data demonstrate that the endonuclease activity of Ercc1-Xpf does not participate in the formation of ICL-induced DSBs. Our data differ from those described in a recent report in which it was demonstrated that Ercc1 mutant CHO cells display a decreased level of γ-H2AX upon treatment with hydroxymethyl-4,5′,8-trimethylpsoralen and UV-A compared to wild-type cells treated similarly (49). This difference may stem from differential processing of monoadducts and ICLs in cells with various degrees of checkpoint response or from different methods of quantitating γ-H2AX. Nevertheless, in our system, in which monoadducts (UV-C) do not induce γ-H2AX foci, MMC did, even in cells in which Ercc1 is genetically deleted.

Interestingly, in both *Ercc1*$^{-/-}$ primary MEFs and ES cells, we detected a higher frequency of spontaneous γ-H2AX foci than in wild-type cells (Fig. 2C versus 1D). This is consistent with the Ercc1-deficient cells' being genomically unstable, which may be a consequence of unrepaired endogenous ICLs. Elevated levels of spontaneous γ-H2AX foci are also observed in tumor cell lines (47), cell lines deficient in the DSB repair proteins DNA-PKcs and NBS1, and cells defective in the DNA damage-signaling molecule ATM (46).

Formation of ICL-induced DSBs requires cell cycle progression, and their repair is slow. Several observations suggest that ICL-induced DSB formation is cell cycle dependent. First, MMC-induced γ-H2AX foci did not begin to accumulate until 6 h after drug exposure (Fig. 1), which may be because MMC must be metabolically activated (19) or ICLs form more slowly than monoadducts (24). However, once MMC-induced γ-H2AX foci began to appear in an asynchronous cell population, an additional 6 h was required before the majority of cells had foci (Fig. 1). Furthermore, only 60% of the cells treated with MMC ever produced foci in the 24-h period following damage. In contrast, γ-H2AX foci appear in all cells within minutes of γ-irradiation (47). Second, rapidly dividing cells are much more sensitive to cross-linking agents than slowly proliferating cells (25, 41, 62). Finally, ICL-induced DSBs occur only in proliferating cultures of *S. cerevisiae* (37). Similarly, in G_1-arrested primary MEFs, MMC did not induce γ-H2AX foci (Fig. 3A), in accordance with a recent study by Rothfuss and Grompe with primary human fibroblasts treated with psoralen (49). However, if the cells were released from their cell cycle block, there was a time-dependent increase in the fraction of cells with foci (Fig. 3B). This result demonstrates that ICL-induced DSB formation in mammalian cells, as in *S. cerevisiae*, requires cell cycle progression.

wild-type cells), 300 nM MMC, or 3.3 μM cisplatin (both equitoxic doses to wild-type cells) for 1 h. (C) Quantitation of γ-H2AX focus formation at various times after exposure of *Ercc1*$^{-/-}$ MEFs to 1 μM MMC. Error bars indicate the standard error of the mean when the data points were collected from more than three individual experiments. (D) Quantitation of γ-H2AX focus formation at various times after exposure of *Xpa*$^{-/-}$ MEFs to 1 μM MMC. (E) Detection of DSBs by pulsed-field gel electrophoresis. Wild-type (wt) and *Ercc1*$^{-/-}$ ES cells were treated for 1 h with 7.2 μM MMC, washed, and incubated for 0 to 48 h more in fresh medium. Plugs of 5×10^6 cells were prepared for each time point and analyzed for low-molecular-weight DNA, indicative of genomic DSBs, by electrophoresis. *Schizosaccharomyces pombe* chromosomes were used as molecular size markers in lane MW.

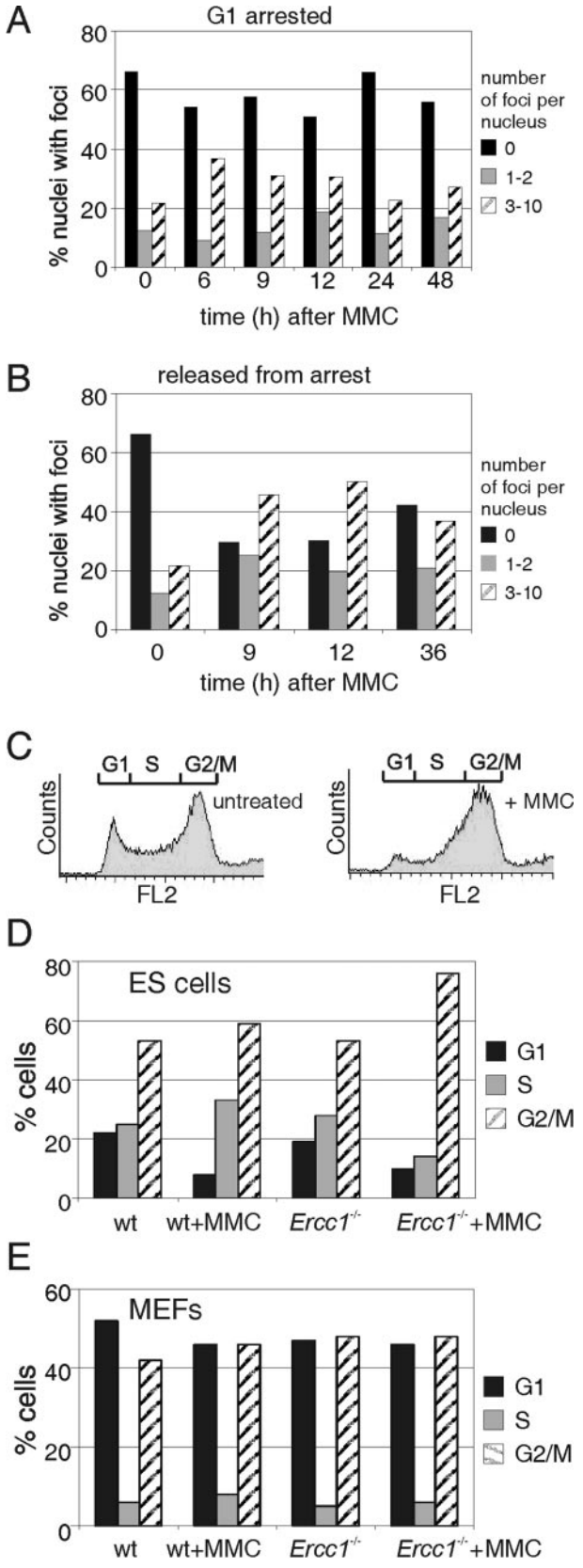

FIG. 3. Relationship between the cell cycle, cross-link damage, and γ-H2AX focus formation. (A) γ-H2AX focus formation after exposure of G_1-arrested wild-type (wt) MEFs to MMC. Early-passage wild-type MEFs were seeded on glass coverslips at a very high density in order to arrest them by contact inhibition. Forty-eight hours later, the cells were exposed to 3 μM MMC for 1 h. At the indicated times after exposure, cells were fixed and immunostained for γ-H2AX. The 12-h sample was done in duplicate. The second replicate was trypsinized 12 h after exposure to MMC, split 1:10 to release the cells from contact inhibition, and reseeded on glass coverslips. The cells were fixed after replating at the times indicated and analyzed as above (B). (C) FACS profile of wild-type ES cells before and after cross-link damage. Genomic DNA of wild-type ES cells was stained with propidium iodide and quantitated by FACS as described in Materials and Methods. Untreated cells were fixed and stained directly. Treated cells were exposed to 3 μM MMC for 1 h, incubated for an additional 12 h, harvested, fixed, and stained. The G_1 (2n DNA content) and G_2/M (4n) fractions of cells are indicated above each profile. (D) Cell cycle distribution of wild-type and *Ercc1*$^{-/-}$ ES cells before and after cross-link damage. Cells were treated as described for panel C. Equitoxic concentrations of MMC were used (3 μM for wild-type cells and 0.3 μM for *Ercc1*$^{-/-}$ cells). The fraction of cells in G_1, S, and G_2/M was determined from the FACS profile and plotted as a percentage of the total. (E) Cell cycle distribution of wild-type and *Ercc1*$^{-/-}$ primary fibroblasts before and after cross-link damage. Cells were treated as described above except that the equitoxic dose of MMC used for *Ercc1*$^{-/-}$ MEFs was 1 μM.

Primary human fibroblasts do not respond to ICL damage by arresting until they reach S phase (2). Furthermore, a site-specific ICL in a double-stranded oligonucleotide is sufficient to block DNA replication and trigger the formation of a DSB in vitro (6). Thus, it is likely that the S phase of the cell cycle is critical for ICL recognition, initiation of repair, and formation of the DSB repair intermediate. FACS analysis of wild-type and *Ercc1*$^{-/-}$ cells 12 h after MMC exposure revealed a strong late S/early G_2 arrest (Fig. 3). Therefore, at the time when the greatest fraction of cells had γ-H2AX foci, the majority of the cells are arrested with ~4n DNA content. DSBs caused by γ-irradiation also trigger an early G_2 arrest (47). These data support the notion that ICL-induced DSBs are incurred during DNA replication.

A striking aspect of ICL-induced γ-H2AX foci is the rate at which they are resolved. The fraction of MMC-treated cells with a large number of foci decreased by only 10% in the 12-h time period following peak focus induction (Fig. 1). In contrast, the number of γ-irradiation-induced γ-H2AX foci declines within 15 min. Sixty percent of γ-irradiation-induced DSBs have a half-life of minutes (45). The relatively slow resolution of ICL-induced DSBs may reflect equilibrium between the rates of DSB formation and repair after MMC-inflicted DNA damage. However, a more likely interpretation is that ICL-induced DSBs are structurally different from γ-irradiation-induced DSBs and are therefore repaired differently. This hypothesis is consistent with genetic data, which indicate a requirement for Ercc1-Xpf for ICL repair but not for more generic DSB repair (10, 42).

ICL-induced DSBs are not repaired in *Ercc1*$^{-/-}$ cells. Quantitation of γ-H2AX foci in *Ercc1*$^{-/-}$ MEFs at different time points after MMC exposure revealed that DSBs arise in the mutant cells with the same kinetics as in wild-type cells. However, once formed, the DSBs are significantly longer-lived in Ercc1-deficient cells. The fraction of cells with γ-H2AX foci did not decrease in the 72-h period following MMC treatment. Furthermore, a greater fraction of *Ercc1*$^{-/-}$ cells than wild-

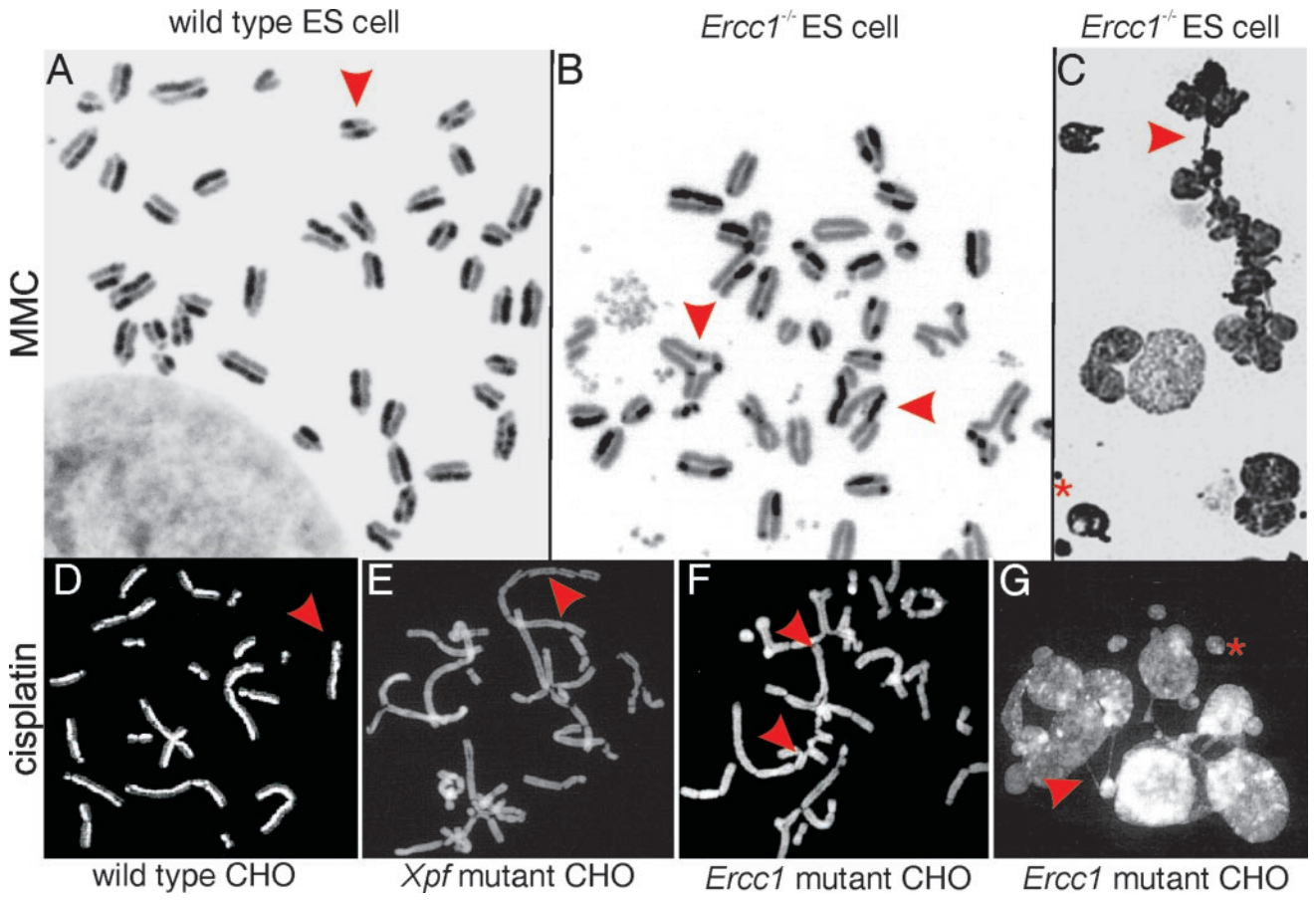

FIG. 4. Analysis of chromosomal aberrations in cells exposed to cross-link damage. Subconfluent cultures of wild-type (wt) and mutant cells were exposed to equitoxic concentrations of MMC or cisplatin for 1 h, washed twice, and then incubated for an additional 24 h in medium containing 10 μg of BrdU per ml. Thirty minutes prior to trypsinization, colcemid was added. (A) A metaphase spread from MMC-treated wild-type ES cells, demonstrating unequal staining of the sister chromatids, indicative of two rounds of DNA replication in the presence of BrdU. Sister chromatid exchanges (arrow) are frequent, but other aberrations are notably absent. (B) Metaphase spread of MMC-treated *Ercc1*$^{-/-}$ ES cell. Aberrations, including gaps, breaks, and radials, were common in mutant cells. Fusions between sister chromatids (indicated with arrows) were the most abundant aberration. (C) Spread of MMC-treated *Ercc1*$^{-/-}$ ES cells, demonstrating anaphase bridging (arrowhead) and micronuclei (asterisk), hallmarks of chromatid nondisjunction and fragmentation, respectively. Furthermore, nuclear size is highly variable, indicating variability in nuclear DNA content. (D) A representative spread from wild-type CHO cells treated with cisplatin, demonstrating frequent sister chromatid exchanges (arrow). (E) A metaphase spread of *Xpf* mutant CHO cells treated with cisplatin. Staining indicates only a single round of replication since drug treatment, and chromatid fusions are abundant (arrows). (F) A metaphase spread from cisplatin-treated *Ercc1* mutant CHO cells, also with numerous fusions (arrows). (G) *Ercc1* mutant CHO cells after cisplatin treatment, with anaphase bridging (arrow) and micronuclei (asterisk).

type cells were in G_2 12 h after exposure to MMC, consistent with an accumulation of mutant cells with unrepaired DNA damage. Thus, Ercc1 plays a role late in ICL repair, after the DSBs are formed. Similar results were reported by de Silva et al., who used pulsed-field gel electrophoresis to detect DSBs in mutant CHO cells reacted with bivalent nitrogen mustards (17). Importantly, MMC-induced γ-H2AX foci did not persist in NER-deficient *Xpa*$^{-/-}$ MEFs, demonstrating that this role of Ercc1-Xpf in ICL repair is independent of NER.

DSBs mediate the toxicity of ICLs. Cells that proliferate more rapidly in culture are more sensitive to chemicals that induce DNA ICLs than slowly proliferating cells (CHO > ES > primary MEF cells) (26, 42, 64). Analogously, we detected a significant G_2 arrest in rapidly growing ES cells but not in slowly proliferating primary MEFs (Fig. 3D and E). Furthermore, cells synchronized in G_2/M do not respond to ICL damage (by arresting or creating DSBs) until they begin traversing the subsequent S phase (2). These data suggest a scenario in which ICLs are first detected during the S phase of the cell cycle. DNA replication triggers the formation of a DSB, which in turn leads to a cell cycle arrest that persists until DSB repair occurs. Thus, the sensitivity of various cell types to cross-linking agents can be predicted based on the extent of their cell cycle arrest, which is in turn determined by their proliferation rate. These data provide experimental evidence for the rationale behind the use of cross-linking agents in cancer chemotherapy, particularly in combination with radiotherapy, as well as an explanation for their toxic side effects in proliferative organs such as the bone marrow and gastrointestinal tract (25). In addition, these data implicate DSBs as the truly toxic lesion after ICL damage.

To explore this further, we examined metaphase spreads of

TABLE 1. Cell cycle arrest and chromosomal aberrations after cross-linking of wild-type and Ercc1-Xpf mutant cells

Cell type	Treatment	No. of metaphases examined	% in first division[a]	% of metaphases with chromatid aberrations[b]	% of metaphases with fusions[c]	% of metaphases with chromosome aberrations[d]
Wild-type ES	None	59	0	0	0	0
	3 μM MMC	57	0	2	0	1
Ercc1$^{-/-}$ ES	None	64	0	20	0	12
	300 nM MMC	114	46	60[e]	46[e]	50[e]
Wild-type CHO	None	50	6	0	0	0
	10 μM cisplatin	47	13	2	13	13
Ercc1 mutant CHO	None	50	10	0	0	2
	1 μM cisplatin	48	100	0	83	62
Xpf mutant CHO	None	50	9	4	0	0
	1 μM cisplatin	47	100	0	92	49

[a] The remainder of the cells had completed a second division in the period following exposure to MMC.
[b] Aberrations restricted to a single chromatid, including gaps, breaks, and radial structures.
[c] Aberrations involving joining of two sister chromatids within a chromosome (ring structure) or different chromosomes (tri- or quadriradials).
[d] Aberrations involving both sister chromatids, including gaps and breaks.
[e] Forty-six percent of these occurred in cells arrested in the first division.

wild-type and mutant ES cells after exposure to MMC (Table 1). In the wild-type ES cells, MMC triggered a high frequency of sister chromatid exchanges (Fig. 4). These exchanges are caused by a DSB in a chromatid that is repaired by homologous recombination with the sister as a template for DNA synthesis (56). Thus, sister chromatid exchanges illustrate the creation and successful repair of DSBs caused by ICLs. Other types of chromosomal aberrations were rare in the wild-type ES cells (Table 1).

In contrast, all of the MMC-treated *Ercc1*$^{-/-}$ ES metaphases from cells arrested in the first division had multiple chromosomal breaks and aberrant structures due to chromatid fusions (Table 1). Mutant cells that progressed to anaphase demonstrated a high frequency of micronuclei and bridging, also a consequence of chromosomal breaks and fusions (Fig. 4C and G). These data provide further evidence that ICL-induced DSBs are more stable in *Ercc1*$^{-/-}$ cells than in wild-type cells, corroborating the γ-H2AX data. The results of the chromosome study in ES cells were recapitulated in CHO cells treated with cisplatin and extended to include an *Xpf* mutant cell line (Table 1, Fig. 4D to G) (15). These data implicate Xpf along with Ercc1 in the resolution of ICL-induced DSBs and thereby likely implicate the endonuclease function of the heterodimer.

Since *Ercc1*$^{-/-}$ ES cells are sensitive to MMC but not γ-irradiation (14, 42) and homologous recombination leading to sister chromatid exchange is possible in *Ercc1*$^{-/-}$ ES cells (Fig. 4C) (42), we conclude that ICL-induced, but not γ-irradiation-induced, DSBs are resistant to homologous recombination until processed by Ercc1-Xpf. One probable difference between γ-irradiation-induced and MMC-induced DSBs is that in the latter, the ICL persists after the creation of the break. Since the DSB is created during the S phase of the cell cycle, the only possibility for DSB repair by homologous recombination demands the creation of a joint molecule between the two recently replicated DNA strands at or near the site of the DSB. An ICL near the DSB would prevent melting of the duplex strands and thereby prevent heteroduplex formation. We propose that Ercc1-Xpf is essential to create a nick near the ICL to make the DNA amenable to DSB repair. In the absence of Ercc1-Xpf, the DSB cannot be repaired by homologous recombination and thus is vulnerable to fusing, which is extremely detrimental to the cell.

Model for ICL repair. Based on these results, we propose a model for the mechanism of DNA ICL repair in mammalian cells that incorporates an essential role for the endonuclease function of Ercc1-Xpf late in the repair reaction (Fig. 5). Our data and those of others suggest that ICL repair is initiated during DNA replication (Fig. 5A) (2; reviewed in reference 38). The ICL prevents the unwinding of the two DNA strands, stalling the replication fork (Fig. 5B). Through the action of a structure-specific endonuclease that is not Ercc1-Xpf but may be Mus81, the stalled fork may be converted to a DSB (6, 8, 11, 32, 36, 62), causing the appearance of γ-H2AX foci. Alternatively, the foci may represent collapsed replication forks. Regardless, stalled replication is required to trigger subsequent events.

Because stalling of the replication fork occurs upstream of the ICL, the resultant DSB is insufficient to remove the damage from the template DNA (Fig. 5C). The formation of a DSB on the leading strand would, however, create a new 3′ end in the template DNA in proximity to the ICL, thereby revealing a substrate for the structure-specific endonuclease Ercc1-Xpf (Fig. 5D) (16). The proposed cleavage by Ercc1-Xpf releases the ICL from one of the two template strands (Fig. 5E). A DSB on the lagging strand (not shown) creates a 5′ end near the ICL. Although this does not create an obvious substrate for Ercc1-Xpf, the endonuclease can nick DNA 3′ to an ICL (29), which would be required to release the ICL from one strand. However, such an incision by Ercc1-Xpf would necessitate single-stranded DNA around the lesion, which may occur if the DSB serves to relieve torsional strain around the ICL.

Once the residual damage is limited to one strand of DNA, it may be bypassed by a DNA polymerase capable of translesion synthesis (Fig. 5F) (37, 66) and subsequently excised from the template strand (Fig. 5G and H), although this is not

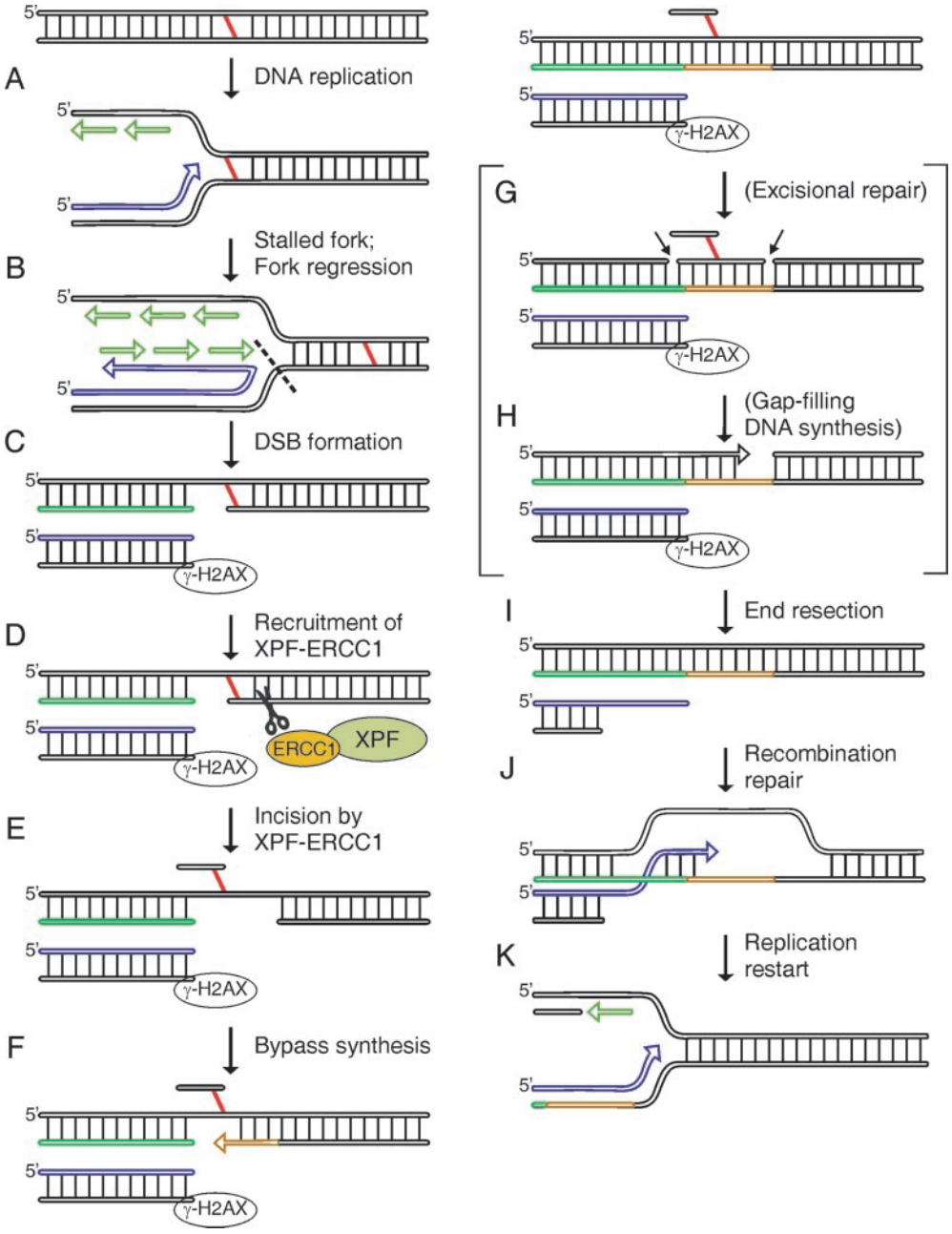

FIG. 5. Model for the mechanism of DNA ICL repair in mammalian cells. The two strands of DNA and their polarity are indicated in black, with vertical lines representing base pairs. A DNA ICL is depicted as a red line connecting the two strands. Newly replicated DNA is depicted with arrows, and for clarity, no base pairing is indicated between the template and the newly synthesized DNA strands. (A) Repair of ICLs is initiated during DNA replication. (B) The ICL prevents the unwinding of the two DNA strands, stalling the replication fork. (C) This leads to fork regression and the formation of a DSB in an Ercc1-Xpf-independent manner. The DSB can be detected as a local accumulation of γ-H2AX by immunostaining. (D) The formation of a DSB creates a substrate for the endonuclease Ercc1-Xpf in the template DNA by revealing a 3′ end near the ICL. (E) Ercc1-Xpf cuts with its characteristic substrate specificity (indicated by scissors). The incision releases the ICL from one of the two DNA strands. (F) The residual DNA damage may be bypassed by a DNA polymerase capable of translesion synthesis (indicated in gold). (G) It may be that residual ICL damage is ultimately excised from the second strand (potential cut sites are indicated with arrows). (H) The resulting gap could be filled by the replication machinery. (I) Repair of the DSB requires resection of the broken end to reveal a 3′ single-stranded overhang. (J) This 3′ end invades the template DNA to create a joint molecule. This is only possible once Ercc1-Xpf has incised the blocking ICL. (K) Expansion of the heteroduplex could enable reestablishment of the replication fork.

essential for resolution of the repair intermediates. Repair of the replication-induced DSB proceeds via homologous recombination (3, 32, 50). Recombination is initiated by invasion of the 3′ end of the DSB, creating a joint molecule with the parental duplex (Fig. 5I and J) (36). Extension of the heteroduplex would enable reestablishment of the replication fork (Fig. 5K).

The proposed model is consistent with an extensive body of

genetic data that implicate proteins involved in homologous recombination, postreplication repair, and the Ercc1-Xpf endonuclease but not other NER proteins in mammalian ICL repair (reviewed in reference 19). In this study, we investigated ICL damage caused by MMC, which causes minimal helix distortion (58), and cisplatin, which causes significant helical distortion (34). Cells treated with either agent behaved identically, with γ-H2AX foci detected after 6 h, cell cycle arrest in late S/G_2, and accumulation of chromosomal aberrations (Fig. 2 and Table 1). Thus, there is no evidence for competing repair reactions. Obviously, if ICLs block DNA replication, they must also impede other DNA metabolic processes that depend upon strand separation, particularly transcription. However, we did not detect an increase in the number of γ-H2AX foci in fibroblasts for up to 48 h after exposure to MMC, making it highly unlikely that interference with RNA polymerase II progression by an ICL results in a DSB (Fig. 3A).

It is interesting to speculate that the recombination-independent and mutation-prone processing of ICLs detected by Zheng et al. in a plasmid-based assay reflects transcription-coupled ICL repair (66). If this is the case, it leads to the prediction that resting cells accumulate point mutations, whereas proliferating cells accumulate chromosomal aberrations as a consequence of ICLs, both of which are observed in vivo as a consequence of ICL damage (30, 57, 65).

ACKNOWLEDGMENTS

This study was supported by grants from the European Union, the Dutch Cancer Society (K.W.F.), and the Netherlands Organization for Scientific Research (NWO). L.J.N. was supported by postdoctoral fellowship PF-99-142 from the American Cancer Society.

REFERENCES

1. **Adair, G. M., R. L. Rolig, D. Moore-Faver, M. Zabelshansky, J. H. Wilson, and R. S. Nairn.** 2000. Role of ERCC1 in removal of long non-homologous tails during targeted homologous recombination. EMBO J. **19:**5552–5561.
2. **Akkari, Y. M., R. L. Bateman, C. A. Reifsteck, S. B. Olson, and M. Grompe.** 2000. DNA replication is required To elicit cellular responses to psoralen-induced DNA interstrand cross-links. Mol. Cell. Biol. **20:**8283–8289.
3. **Arnaudeau, C., C. Lundin, and T. Helleday.** 2001. DNA double-strand breaks associated with replication forks are predominantly repaired by homologous recombination involving an exchange mechanism in mammalian cells. J. Mol. Biol. **307:**1235–1245.
4. **Bardwell, A. J., L. Bardwell, A. E. Tomkinson, and E. C. Friedberg.** 1994. Specific cleavage of model recombination and repair intermediates by the yeast Rad1-Rad10 DNA endonuclease. Science **265:**2082–2084.
5. **Berardini, M., W. Mackay, and E. L. Loechler.** 1997. Evidence for a recombination-independnet pathway for the repair of DNA interstrand cross-links on a site-specific study with nitrogen mustard. Biochemistry **36:**3506–3513.
6. **Bessho, T.** 2003. Induction of DNA replication-mediated double strand breaks by psoralen DNA interstrand cross-links. J. Biol. Chem. **278:**5250–5254.
7. **Biggerstaff, M., D. E. Szymkowski, and R. D. Wood.** 1993. Co-correction of the ERCC1, ERCC4 and xeroderma pigmentosum group F DNA repair defects in vitro. EMBO J. **12:**3685–3692.
8. **Boddy, M. N., P. H. Gaillard, W. H. McDonald, P. Shanahan, J. R. Yates, 3rd, and P. Russell.** 2001. Mus81-Eme1 are essential components of a Holliday junction resolvase. Cell **107**:537–548.
9. **Bredberg, A., B. Lambert, and S. Soderhall.** 1982. Induction and repair of psoralen cross-links in DNA of normal human and xeroderma pigmentosum fibroblasts. Mutat. Res. **93:**221–234.
10. **Busch, D. B., H. van Vuuren, J. de Wit, A. Collins, M. Z. Zdzienicka, D. L. Mitchell, K. W. Brookman, M. Stefanini, R. Riboni, L. H. Thompson, R. B. Albert, A. J. van Gool, and J. H. J. Hoeijmakers.** 1997. Phenotypic heterogeneity in nucleotide excision repair mutants of rodent complementation groups 1 and 4. Mutat. Res. **383:**91–106.
11. **Chen, X. B., R. Melchionna, C. M. Denis, P. H. Gaillard, A. Blasina, I. Van de Weyer, M. N. Boddy, P. Russell, J. Vialard, and C. H. McGowan.** 2001. Human Mus81-associated endonuclease cleaves Holliday junctions in vitro. Mol. Cell **8:**1117–1127.
12. **Dardalhon, M., and D. Averbeck.** 1995. Pulsed-field gel electrophoresis analysis of the repair of psoralen plus UVA induced DNA photoadducts in Saccharomyces cerevisiae. Mutat. Res. **336:**49–60.
13. **Dardalhon, M., B. de Massy, A. Nicolas, and D. Averbeck.** 1998. Mitotic recombination and localized DNA double-strand breaks are induced after 8-methoxypsoralen and UVA irradiation in Saccharomyces cerevisiae. Curr. Genet. **34:**30–42.
14. **Darroudi, F., and A. T. Natarajan.** 1985. Cytological characterization of repair-deficient CHO cell line 43–3B. I. Induction of chromosomal aberrations and sister-chromatid exchanges by UV and its modulation with 3-aminobenzamide. Mutat. Res. **149:**239–247.
15. **Darroudi, F., A. T. Natarajan, and P. H. M. Lohman.** 1989. Cytogenetical characterization of the UV-sensitive repair-deficient CHO cell line 43–3B: II. Induction of cell killing, chromosomal aberrations and sister-chromatid exchanges by 4NQO, mono- and bi-functional alkylating agents. Mutat. Res. **212:**103–112.
16. **de Laat, W. L., E. Appeldoorn, N. G. Jaspers, and J. H. J. Hoeijmakers.** 1998. DNA structural elements required for ERCC1-XPF endonuclease activity. J. Biol. Chem. **273:**7835–7842.
17. **De Silva, I. U., P. J. McHugh, P. H. Clingen, and J. A. Hartley.** 2000. Defining the roles of nucleotide excision repair and recombination in the repair of DNA interstrand cross-links in mammalian cells. Mol. Cell. Biol. **20:**7980–7990.
18. **de Vries, A., C. T. van Oostrom, P. M. Dortant, R. B. Beems, C. F. van Kreijl, P. J. Capel, and H. van Steeg.** 1997. Spontaneous liver tumors and benzo-[a]pyrene-induced lymphomas in XPA-deficient mice. Mol. Carcinog. **19:**46–53.
19. **Dronkert, M., and R. Kanaar.** 2001. Repair of DNA interstrand cross-links. Mutat. Res. **486:**217–247.
20. **Dronkert, M. L. G., H. B. Beverloo, R. D. Johnson, J. H. J. Hoeijmakers, M. Jasin, and R. Kanaar.** 2000. Mouse RAD54 affects DNA double-strand break repair and sister chromatid exchange. Mol. Cell. Biol. **20:**3147–3156.
21. **Fishman-Lobell, J., and J. E. Haber.** 1992. Removal of nonhomologous DNA ends in double-strand break recombination: the role of the yeast ultraviolet repair gene. RAD1. Science. **258:**480–484.
22. **Flores-Rozas, H., and R. D. Kolodner.** 2000. Links between replication, recombination and genome instability in eukaryotes. Trends Biochem. Sci. **25:**196–200.
23. **Grossmann, K. F., A. M. Ward, M. E. Matkovic, A. E. Folias, and R. E. Moses.** 2001. S. cerevisiae has three pathways for DNA interstrand crosslink repair. Mutat. Res. **487:**73–83.
24. **Hartley, J. A., M. D. Berardini, and R. L. Souhami.** 1991. An agarose gel method for the determination of DNA interstrand crosslinking applicable to the measurement of the rate of total and "second-arm" crosslink reactions. Anal. Biochem. **193:**131–134.
25. **Hartmann, J. T., C. Kollmannsberger, L. Kanz, and C. Bokemeyer.** 1999. Platinum organ toxicity and possible prevention in patients with testicular cancer. Int. J. Cancer **83:**866–869.
26. **Hoy, C. A., L. H. Thompson, C. L. Mopney, and E. P. Salazar.** 1985. Defective DNA cross-link removal in Chinese hamster cell mutants hypersensitive to bifunctional alkylating agents. Cancer Res. **45:**1737–1743.
27. **Klein, H. L.** 1988. Different types of recombination events are controlled by the *RAD1* and *RAD52* genes of *Saccharomyces cerevisiae*. Genetics **120:**367–377.
28. **Krempler, A., M. D. Henry, A. A. Triplett, and K. U. Wagner.** 2002. Targeted deletion of the Tsg101 gene results in cell cycle arrest and G2/S and p53-independent cell death. J. Biol. Chem. **277:**43216–43223.
29. **Kuraoka, I., W. R. Kobertz, R. R. Ariza, M. Biggerstaff, J. M. Essigmann, and R. D. Wood.** 2000. Repair of an interstrand DNA cross-link initiated by ERCC1-XPF repair/recombination nuclease. J. Biol. Chem. **275:**26632–26636.
30. **Laquerbe, A., C. Guillouf, E. Moustacchi, and D. Papadopoulo.** 1995. The mutagenic processing of psoralen photolesions leaves a high specific signature at an endogenous human locus. J. Mol. Biol. **254:**38–49.
31. **Lawley, P. D., and D. H. Phillips.** 1996. DNA adducts from chemotherapeutic agents. Mutat. Res. **355:**13–40.
32. **Lundin, C., K. Erixon, C. Arnaudeau, N. Schultz, D. Jenssen, M. Meuth, and T. Helleday.** 2002. Different roles for nonhomologous end joining and homologous recombination following replication arrest in mammalian cells. Mol. Cell. Biol. **22:**5869–5878.
33. **Magana-Schwencke, N., J. A. Henriques, R. Chanet, and E. Moustacchi.** 1982. The fate of 8-methoxypsoralen photoinduced crosslinks in nuclear and mitochondrial yeast DNA: comparison of wild-type and repair-deficient strains. Proc. Natl. Acad. Sci. USA **79:**1722–1726.
34. **Malinge, J. M., M. J. Giraud-Panis, and M. Leng.** 1999. Interstrand cross-links of cisplatin induce striking distortions in DNA. J. Inorg. Biochem. **77:**23–29.
35. **Matsunaga, T., D. Mu, C. H. Park, J. T. Reardon, and A. Sancar.** 1995. Human DNA repair excision nuclease. Analysis of the roles of the subunits involved in dual incisions by using anti-XPG and anti-ERCC1 antibodies. J. Biol. Chem. **270:**20862–20869.

36. **McGlynn, P., and R. G. Lloyd.** 2002. Recombinational repair and restart of damaged replication forks. Nat. Rev. Mol. Cell. Biol. **3:**859–870.
37. **McHugh, P. J., W. R. Sones, and J. A. Hartley.** 2000. Repair of intermediate structures produced at DNA interstrand cross-links in *Saccharomyces cerevisiae*. Mol. Cell. Biol. **20:**3425–3433.
38. **McHugh, P. J., V. J. Spanswick, and J. A. Hartley.** 2001. Repair of DNA interstrand crosslinks: molecular mechanisms and clinical relevance. Lancet Oncol. **2:**483–490.
39. **Mirzoeva, O. K., and J. H. Petrini.** 2003. DNA replication-dependent nuclear dynamics of the Mre11 complex. Mol. Cancer Res. **1:**207–218.
40. **Modesti, M., and R. Kanaar.** 2001. DNA repair: spot(light)s on chromatin. Curr. Biol. **11:**R229–R232.
41. **Mu, D., C.-H. Park, T. Matsunaga, D. S. Hsu, J. T. Reardon, and A. Sancar.** 1995. Reconstitution of human DNA repair excision nuclease in a highly defined system. J. Biol. Chem. **270:**2415–2418.
42. **Niedernhofer, L. J., J. Essers, G. Weeda, B. Beverloo, J. de Wit, M. Muijtjens, H. Odijk, J. H. Hoeijmakers, and R. Kanaar.** 2001. The structure-specific endonuclease Ercc1-Xpf is required for targeted gene replacement in embryonic stem cells. EMBO J. **20:**6540–6549.
43. **O'Connor, P. M., and K. W. Kohn.** 1990. Comparative pharmacokinetics of DNA lesion formation and removal following treatment of L1210 cells with nitrogen mustards. Cancer Commun. **2:**387–394.
44. **Palom, Y., G. Suresh Kumar, L. Q. Tang, M. M. Paz, S. M. Musser, S. Rockwell, and M. Tomasz.** 2002. Relative toxicities of DNA cross-links and monoadducts: new insights from studies of decarbamoyl mitomycin C and mitomycin C. Chem. Res. Toxicol. **15:**1398–1406.
45. **Paques, F., and J. E. Haber.** 1997. Two pathways for removal of nonhomologous DNA ends during double-strand break repair in *Saccharomyces cerevisiae*. Mol. Cell. Biol. **17:**6765–6771.
46. **Paull, T. T., E. P. Rogakou, V. Yamazaki, C. U. Kirchgessner, M. Gellert, and W. M. Bonner.** 2000. A critical role for histone H2AX in recruitment of repair factors to nuclear foci after DNA damage. Curr. Biol. **10:**886–895.
47. **Rogakou, E. P., C. Boon, C. Redon, and W. M. Bonner.** 1999. Megabase chromatin domains involved in DNA double-strand breaks in vivo. J. Cell Biol. **146:**909–915.
48. **Rogakou, E. P., D. R. Pilch, A. H. Orr, V. S. Ivanova, and W. M. Bonner.** 1998. DNA Double-stranded breaks induce histone H2AX phosphorylation on serine 139. J. Biol. Chem. **273:**5858–5868.
49. **Rothfuss, A., and M. Grompe.** 2004. Repair kinetics of genomic interstrand DNA cross-links: evidence for DNA double-strand break-dependent activation of the Fanconi anemia/BRCA pathway. Mol. Cell. Biol. **24:**123–134.
50. **Saintigny, Y., F. Delacote, G. Vares, F. Petitot, S. Lambert, D. Averbeck, and B. S. Lopez.** 2001. Characterization of homologous recombination induced by replication inhibition in mammalian cells. EMBO J. **20:**3861–3870.
51. **Sargent, R. G., J. L. Meservy, B. D. Perkins, A. E. Kilburn, Z. Intody, G. M. Adair, R. S. Nairn, and J. H. Wilson.** 2000. Role of the nucleotide excision repair gene ERCC1 in formation of recombination-dependent rearrangements in mammalian cells. Nucleic Acids Res. **28:**3771–3778.
52. **Schiestl, R. H., and S. Prakash.** 1988. *RAD1*, an excision repair gene of *Saccharomyces cerevisiae*, is also involved in recombination. Mol. Cell. Biol. **8:**3619–3626.
53. **Schiestl, R. H., and S. Prakash.** 1990. *RAD10*, an excision repair gene of *Saccharomyces cerevisiae*, is involved in the *RAD1* pathway of mitotic recombination. Mol. Cell. Biol. **10:**2485–2491.
54. **Sijbers, A. M., P. J. van der Spek, H. Odijk, J. van den Berg, M. van Duin, A. Westerveld, N. G. Jaspers, D. Bootsma, and J. H. Hoeijmakers.** 1996. Mutational analysis of the human nucleotide excision repair gene ERCC1. Nucleic Acids Res. **24:**3370–3380.
55. **Sladek, F., M. Munn, W. Rupp, and P. Howard-Flanders.** 1989. In vitro repair of psoralen-DNA cross-links by RecA, UvrABC, and the 5′-exonuclease of DNA polymerase I. J. Biol. Chem. **264:**6755–6765.
56. **Sonoda, E., M. S. Sasaki, C. Morrison, Y. Yamaguchi-Iwai, M. Takata, and S. Takeda.** 1999. Sister chromatid exchanges are mediated by homologous recombination in vertebrate cells. Mol. Cell. Biol. **19:**5166–5169.
57. **Takeiri, A., M. Mishima, K. Tanaka, A. Shioda, O. Ueda, H. Suzuki, M. Inoue, K. Masumura, and T. Nohmi.** 2003. Molecular characterization of mitomycin C-induced large deletions and tandem-base substitutions in the bone marrow of gpt delta transgenic mice. Chem. Res. Toxicol. **16:**171–179.
58. **Tomasz, M., R. Lipman, D. Chowdary, J. Pawlak, G. L. Verdine, and K. Nakanishi.** 1987. Isolation and structure of a covalent cross-link adduct between mitomycin C and DNA. Science **235:**1204–1208.
59. **van Vuuren, A. J., E. Appeldoorn, H. Odijk, A. Yasui, N. G. J. Jaspers, D. Bootsma, and J. H. J. Hoeijmakers.** 1993. Evidence for a repair enzyme complex involving ERCC1 and complementing activities of ERCC4, ERCC11 and xeroderma pigmentosum group F. EMBO J. **12:**3693–3701.
60. **Volker, M., M. J. Mone, P. Karmakar, A. van Hoffen, W. Schul, W. Vermeulen, J. H. Hoeijmakers, R. van Driel, A. A. van Zeeland, and L. H. Mullenders.** 2001. Sequential assembly of the nucleotide excision repair factors in vivo. Mol. Cell **8:**213–224.
61. **Wakasugi, M., J. T. Reardon, and A. Sancar.** 1997. The non-catalytic function of XPG protein during dual incision in human nucleotide excision repair. J. Biol. Chem. **272:**16030–16034.
62. **Ward, I. M., and J. Chen.** 2001. Histone H2AX is phosphorylated in an ATR-dependent manner in response to replicational stress. J. Biol. Chem. **276:**47759–47762.
63. **Warren, A. J., D. J. Mustra, and J. W. Hamilton.** 2001. Detection of mitomycin C-DNA adducts in human breast cancer cells grown in culture, as xenografted tumors in nude mice, and in biopsies of human breast cancer patient tumors as determined by ^{32}P-postlabeling. Clin. Cancer Res. **7:**1033–1042.
64. **Weeda, G., I. Donker, J. de Wit, H. Morreau, R. Janssens, C. J. Vissers, A. Nigg, H. van Steeg, D. Bootsma, and J. H. J. Hoeijmakers.** 1997. Disruption of mouse ERCC1 results in a novel repair syndrome with growth failure, nuclear abnormalities and senescence. Curr. Biol. **7:**427–439.
65. **Wijen, J., M. Nivard, and E. Vogel.** 2000. The in vivo genetic activity profile of the monofunctional nitrogen mustard 2-chlorethamine differs drastically from its bifunctional counterpart mechlorethamine. Carcinogenesis **21:**1859–1867.
66. **Zheng, H., X. Wang, A. J. Warren, R. J. Legerski, R. S. Nairn, J. W. Hamilton, and L. Li.** 2003. Nucleotide excision repair- and polymerase eta-mediated error-prone removal of mitomycin C interstrand cross-links. Mol. Cell. Biol. **23:**754–761.